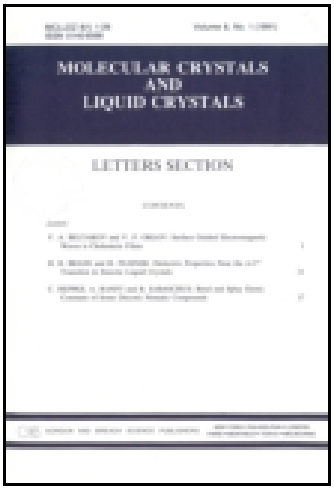

Molecular Crystals and Liquid Crystals
Publication details, including instructions for authors and subscription information:
http://www.tandfonline.com/loi/gmcl20

Diketopyrrolopyrrole-based Small Molecule for Application in Solution Processed Organic Solar Cells

Mi Young Jo[a], Jong Hyun Park[a], Gyeong Eun Lim[a], Jeong Ho Cho[b], Seong Soo Park[c], Seong-Soo Hong[d] & Joo Hyun Kim[a]

[a] Department of Polymer Engineering, Pukyong National University, Busan, Korea

[b] SKKU Advanced Institute of Nanotechnology (SAINT), Sungkyunkwan University, Suwon, Korea

[c] Department of Industrial Chemistry, Pukyong National University, Busan, Korea

[d] Department of Chemical Engineering, Pukyong National University, Busan, Korea

Published online: 17 Nov 2014.

To cite this article: Mi Young Jo, Jong Hyun Park, Gyeong Eun Lim, Jeong Ho Cho, Seong Soo Park, Seong-Soo Hong & Joo Hyun Kim (2014) Diketopyrrolopyrrole-based Small Molecule for Application in Solution Processed Organic Solar Cells, Molecular Crystals and Liquid Crystals, 598:1, 111-119, DOI: 10.1080/15421406.2014.933382

To link to this article: http://dx.doi.org/10.1080/15421406.2014.933382

Mol. Cryst. Liq. Cryst., Vol. 598: pp. 111–119, 2014

ISSN: 1542-1406 print/1563-5287 online
DOI: 10.1080/15421406.2014.933382

Diketopyrrolopyrrole-based Small Molecule for Application in Solution Processed Organic Solar Cells

MI YOUNG JO,[1] JONG HYUN PARK,[1] GYEONG EUN LIM,[1] JEONG HO CHO,[2] SEONG SOO PARK,[3] SEONG-SOO HONG,[4] AND JOO HYUN KIM[1,*]

[1]Department of Polymer Engineering, Pukyong National University, Busan, Korea
[2]SKKU Advanced Institute of Nanotechnology (SAINT), Sungkyunkwan University, Suwon, Korea
[3]Department of Industrial Chemistry, Pukyong National University, Busan, Korea
[4]Department of Chemical Engineering, Pukyong National University, Busan, Korea

A novel donor-π bridge - acceptor (A)-π bridge - donor type molecule (PCTDPP20) with planar core based on diketopyrrolopyrrole (DPP) and carbazole is synthesized by the Suzuki coupling reaction. We introduce phenyl rings to extend the π-conjugation length as a π-bridge. The HOMO and LUMO energy levels of PCTDPP20 are −5.13 and −3.57 eV, respectively. From the UV-Vis spectra, we confirm that the maximum absorption wavelgth (λ_{max}) of the PCTDPP20 annealed film at 100°C is red-shifted about 30 nm and the absorption intensity at 600 ∼ 650 nm increase compared to that of as-spun film. And the OFET based on PCTDPP20 annealed at 100°C exhibits a highest hole mobility of 1.6 × 10^{-4} cm^2/Vs together with a I_{on}/I_{off} ratio of 1.0 × 10^4 and a V_{th} of 14 V. Also, the photovoltaic properties are investigated in the device structure of ITO/PEDOT:PSS/PCTDPP20:PC_{60}BM (with different blend ratios)/Al. Among the OSCs, PCTDPP20:PCBM weight ratio of 1:0.8 and termal annealing process at 100°C for 10 min are optimum belnd ratio and temperature, respectively. This device shows the best performance with a highest PCE of 0.95% a J_{sc} of −2.69 mA/cm^2, a V_{oc} of 0.79 V and a fill factor of 44.5%.

Keywords Organic solar cells; organic field effect transistors; diketopyrrolopyrrole; carbazole; solution process.

1. Introduction

Organic solar cells (OSCs) have been studied on account of many advantages of thickness, flexibility, process, light weight, and so on [1]. Nowadays, power conversion efficiency (PCE) of OSCs reached about 9%, by using low band gap polymers as a donor [2]. Although

*Address correspondence to J. H. Kim, Department of Polymer Engineering, Pukyong National University, Yongdang-Dong, Nam-Gu, Busan 608-739, Korea (ROK). Tel.: (+82)51-629-6452; Fax: (+82)51-629-6429nh. E-mail: jkim@pknu.ac.kr

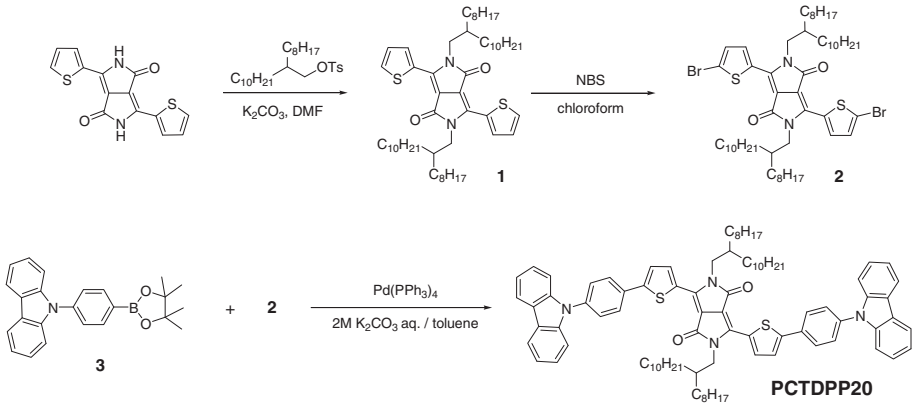

Scheme 1. Synthesis route of the PCTDPP20.

high PCEs were reported in polymer bulk heterojunction (BHJ) solar cells, polymers have batch to batch variations in polydispersity, molecular weight, solubility and others. On this account, small molecules have been attracting great attention recently due to their advantages, i.e., monodisperse nature, reproducibility, high molecular purity and scalable synthesis [3–6]. Small molecular organic semiconductors also show higher carrier mobility than polymeric counterparts because they are more likely to exhibit long-range order [4]. However, most of small molecules show still low PCE in OSCs as a result of inferior film quality of small molecule devices using solution process as compared with polymeric counterparts [7]. To get higher PCE in small molecule solar cells, it is necessary to study on novel molecules with characteristics such as low band gap, good film morphology, high carrier mobility and so on.

The diketopyrrolopyrrole (DPP) has emerged as a promising unit in electronic devices such as OSCs [8] and organic field effect transistors (OFETs) [9]. The DPP derivatives exhibit high carrier mobility of $\sim$2 cm^2/Vs by strong π-π stacking of the DPP-based materials result from a planar bicycle structure [4, 10]. Also the DPP based materials are applicable to soluble process because they are easy to introduce alkyl chain on 3,4-position for getting solubility [11]. Additionally, D-A type materials based on DPP show narrow band gap by strong electron withdrawing ability [8]. To date, polymeric material based DPP solar cell devices exhibit PCEs of 6.5% [12].

With the benefits of small molecule and DPP unit, a D (donor) -π-A (acceptor) -π-D (donor) type small molecule PCTDPP20 (shown in the Scheme 1) based on DPP and carbazole derivatives was synthesized. To confirm characteritics of the PCTDPP20, we fabricated OFETs and OSCs through solution process. After thermal annealing process, performances of the devices was comprehensive improved. In this paper, we investigated the optical, electrochemical, field effect transistor and photovoltaic properties of the PCTDPP20.

2. Experimental Section

2.1. Materials and Synthesis

3,6-bis(5-bromothiophen-2-yl)-2,5-bis(2-octyldodecyl)pyrrolo[3,4-c]pyrrole-1,4(2*H*,5*H*)-dione [13], 2-octyldodecyl 4-methylbenzenesulfonate [14] and 9-(4-(4,4,5,5-tetramethyl-1,

3,2-dioxaborolan-2-yl)phenyl)-9*H*-carbazole [15] were prepared by the literature procedures. And the other chemicals were purchased from Sigma-Aldrich Co, Tokyo Chemical Industry (TCI) or Alfa Aesar (A Johnson Matthey Company) and used as-received without further purification unless otherwise described.

*2.1.1. 2,5-bis(2-octyldodecyl)-3,6-di(thiophen-2-yl)pyrrolo[3,4-c]pyrrole-1,4(*2H,5H*)-dione (1).* This compound obtained by the reaction between 0.3 g (1 mmol) of 3,6-Dithiophen-2-yl-2,5-dihydro-pyrrolo[3,4-c]pyrrole-1,4-dione and 0.95 g (2.1 mmol) of 2-octyldodecyl 4-methylbenzenesulfonate in K_2CO_3 (1.38 g, 10 mmol)/DMF (40 mL). The yield of dark-red solid was 0.069 g (8.1%). mp: 70.6°C. ^{1}H-NMR (400 MHz, $CDCl_3$, ppm): δ 8.86 ~ 8.84 (dd, $J_1 = 4.04$ Hz, $J_2 = 1.08$ Hz, 2H), 7.60 ~ 7.59 (dd, $J_1 = 5.12$ Hz, $J_2 = 1.08$ Hz, 2H), 7.25 ~ 7.24 (d, $J = 4.04$ Hz, 2H), 4.01 ~ 3.99 (d, $J = 7.72$ Hz, 4H), 1.19 (s, 60H), 0.87 ~ 0.82 (m, 18H). Anal. Calcd. for $C_{54}H_{88}N_2O_2S_2$: C, 75.29; H, 10.30; N, 3.25; O, 3.71; S, 7.44. Found: C, 75.5; H, 10.1; N, 3.32; S, 7.38.

*2.1.2. 3,6-bis(5-bromothiophen-2-yl)-2,5-bis(2-octyldodecyl)pyrrolo[3,4-c]pyrrole-1,4(*2H*,* 5H*)-dione (2).* This compound obtained by the reaction between 0.187 g (1.05 mmol) of NBS and (0.431 g, 0.5 mmol) of compound **1** in 50 mL of $CHCl_3$. The yield of dark-red solid was 0.358 g (70.3%). ^{1}H-NMR (400 MHz, $CDCl_3$, ppm): δ 8.62 ~ 8.60 (d, $J = 4.40$ Hz, 2H), 7.20 ~ 7.19 (d, $J = 4.04$ Hz, 2H), 3.91 ~ 3.89 (d, $J = 7.68$ Hz, 4H), 1.57 (s, 20H), 1.26 (s, 18H), 0.87 ~ 0.82 (m, 40H). Anal. Calcd. for $C_{54}H_{86}Br_2N_2O_2S_2$: C, 63.64; H, 8.50; Br, 15.68; N, 2.75; O, 3.14; S, 6.29. Found: C, 63.5; H, 8.49; N, 2.78; S, 6.41.

*2.1.3. 9-(4-(4,4,5,5-tetramethyl-1,3,2-dioxaborolan-2-yl)phenyl)-9*H*-carbazole (3).* This compound obtained by the reaction between 5.00 g (15.5 mmol) of 9-(4-bromophenyl)-9*H*-carbazole and 7.88 g (31.1 mmol) of bis(pinacolato)diboron in the presence of Pd(dppf)Cl_2 0.634 g (0.776 mmol) in potassium acetate 9.14 g (93.1 mmol)/DMF (50 mL). The yield of white crystal was 4.69 g (82.0%). ^{1}H-NMR (400 MHz, $CDCl_3$, ppm): 8.14 ~ 8.12 (d, $J = 7.68$ Hz, 2H), 8.05 ~ 8.03 (d, $J = 8.04$ Hz, 2H), 7.59 ~ 7.57 (d, $J = 8.40$ Hz, 2H), 7.45 ~ 7.37 (m, 4H), 7.29 ~ 7.26 (t, $J = 7.70$ Hz, 2H), 1.39 (s, 12H). Anal. Calcd. for $C_{24}H_{24}BNO_2$: C, 78.06, H, 6.55, B, 2.93, N, 3.79, O, 8.67. Found: C, 77.9, H, 6.52, N, 3.82.

*2.1.4. 3,6-bis(5-(4-(9*H*-carbazol-9-yl)phenyl)thiophen-2-yl)-2,5-bis(2-octyldodecyl)pyrrolo[3,4-c]pyrrole-1,4(*2H,5H*)-dione (PCTDPP20).* PCTDPP20 was synthesized by the general procedure [16] of the Suzuki coupling reaction between compound 2 (0.204 g, 0.2 mmol) and compound 3 (0.163 g, 0.44 mmol). The yield of light yellow solid was 237 mg (88.0%). ^{1}H-NMR (400 MHz, $CDCl_3$, ppm): δ 8.99 ~ 8.98 (d, $J = 4.04$ Hz, 2H), 8.16 ~ 8.14 (d, $J = 8.72$ Hz, 4H), 7.92 ~ 7.89 (d, $J = 12.1$ Hz, 4H), 7.66 ~ 7.64 (d, $J = 8.72$ Hz, 4H), 7.57 ~ 7.56 (d, $J = 4.40$ Hz, 2H), 7.48 ~ 7.41 (m, 8H), 7.32 ~ 7.28 (t, $J = 7.60$ Hz, 4H), 4.12 ~ 4.10 (d, $J = 6.10$ Hz, 4H), 1.37 (s, 20H), 1.29 ~1.24 (m, 28H), 0.89 ~ 0.81 (m, 30H). Anal. Calcd. for $C_{90}H_{110}N_4O_2S_2$: C, 80.43; H, 8.25; N, 4.17; O, 2.38; S, 4.77. Found: C, 81.1; H, 8.22; N, 4.18; S, 4.83.

2.2. Measurements

Synthesized compounds were characterized by ^{1}H-NMR spectra, which were obtained with a JEOL JNM ECP-400 spectrometer. The elemental analyses of synthesized compounds

were carried out an Elementar Vario macro/micro elemental analyzer. UV-Visible (UV-Vis) spectra were recorded using a JASCO V-530 Spectrophotometer. And cyclic voltammograms were performed by an Ivium B14406 with a three electrode cell in a solution of 0.10 M tetrabutylammonium hexafluorophosphate (Bu_4NPF_6) in anhydrous acetonitrile at a scan rate of 100 mV/s. Pt coil and wire were used as the counter and working electrode, and an Ag/Ag^+ electrode was used as the reference electrode. Prior to each measurement, the cell was deoxygenated with nitrogen and the PCTDPP20 was dip-coated on the working electrode. The J–V measurements of the solar cells under the 1.0 sun (100 mW/cm^2) condition from a 150 W Xe lamp with AM 1.5G filter were performed using a KEITHLEY Model 2400 source-measure unit. A calibrated Si reference cell with a KG5 filter certified by National Institute of Advanced Industrial Science and Technology was used to confirm 1.0 sun condition.

2.3. Fabrication of OSCs

ITO-coated on glass substrates were cleaned with deionized water, acetone, methanol, isopropanol in ultrasonic bath. First, OSCs were fabricated through the conventional process. A layer (∼40 nm) of diluted PEDOT:PSS (Clevios P) with isopropanol (PEDOT:PSS:isopropanol = 1:2 by volume) was spin-coated on pre-cleaned ITO substrate (sheet resistance = 15 Ω/sq) which was pre-treated by UV/O_3 for 120 sec. After being baked at 150°C for 10 min under the air, the active layer was spin-cast from the blend solution of PCTDPP20/$PC_{60}BM$ at 1000 rpm for 60 s. The blend of PCTDPP20 (weight of PCTDPP20 was kept 10 mg) and $PC_{60}BM$ with various weight ratio (0.8:1, 1:1, 1:0.8 w/w) was dissolved in 1 mL of chloroform. The blended solution was stirred for overnight at 40°C in the glove box. Prior to spin coating, the blend solution was filtered through a 0.20-μm of PTFE membrane filter. Finally, an 110 nm-thick Al electrodes were deposited by thermal evaporation at 2×10^{-6} Torr. Thermal annealing process was carried out on hot plate in a glove box filled with nitrogen gas. The typical active area of the devices was 13 mm^2.

2.4. Fabrication of Organic Field Effect Transistors

OFETs were built on heavily-doped n-type Si substrates, which are commonly used as gate electrodes. A thermally-grown 300 nm-thick SiO_2 layer served as the gate dielectric. Prior to treating the silicon oxide surface, the wafers were cleaned in piranha solution for 30 min and washed with deionized water, acetone, and isopropanol. The capacitance of the SiO_2 gate dielectric was 11.5 nF/cm^2. The PCTDPP20 film was spin-coated from a 15 mg/mL of chloroform solution onto the SiO_2/Si substrate. Thermal annealing process was carried out on hot plate in a glove box filled with nitrogen gas. Finally, a 50 nm-thick Au source/drain electrodes were thermally evaporated through the shadow masks. The length and width of channels were 100 and 8000 μm, respectively.

3. Results and Discussion

Scheme 1 shows the synthesis route for solution-processible small molecule (PCTDPP20), which was synthesized by the well-known palladium-catalyzed Suzuki coupling reaction. The two 2-octyl dodecyl side chains on DPP were used to improve the solubility in organic solvents. Also phenyl rings were introduced to extend the π-conjugation length and absorb

Table 1. Summary of optical and electrochemical properties

Small molecule	Solution λ_{max} (nm)[a]	Film λ_{max} (nm)[b] / E_g^{opt} (eV)[d]	Film λ_{max} (nm)[c] / E_g^{opt} (eV)[d]	E_{ox} (V)[e] / E_{HOMO} (eV)	E_{red} (V)[e] / E_{LUMO} (eV)	E_g^{elec} (eV)[f]
PCTDPP20	601	577 / 1.77	604 / 1.72	0.44, 0.83 / −5.13	−1.54, −2.01 / −3.57	1.56

[a] measured in a chloroform solution. [b] as-cast spin-coated film from a chloroform. [c] after annealing at 100°C for 10 min. [d] optical band gap (E_g^{opt}). [e] potential determined by CV in 0.10 M Bu_4NPF_6/CH_3CN. [f] electrochemical band gap (E_g^{elec}).

longer wavelength region [17]. The PCTDPP20 was soluble in organic solvents such as methylene chloride, chloroform, toluene and dichlorobenzene.

Figure 1 shows the UV-Vis spectra of the PCTDPP20 in chloroform solution, as-cast film, annealed at 100°C and 150°C for 10 min, respectively. The UV-Vis spectra of those are distinguished at 500 ∼ 700 nm, which is ascribed to the intramolecular charge transfer (ICT) band created by DPP and carbazole unit [3, 18]. The maximum absorption wavelength (λ_{max}) of thin film is blue shifted about 30 nm than that of solution in chloroform. The absorption spectrum in thin film shows a new shoulder peak at 640 ∼ 720 nm, which may be caused by the existence of π-π stacking [5, 19]. After annealing process, the absorption band at 565 – 590 nm is red-shifted about 30 nm and the intensity of shoulder peak increase than those of as-cast film. It is indicating that annealing process is influence of π-π stacking. The temperature of annealing processes at 100°C and 150°C make no great difference.

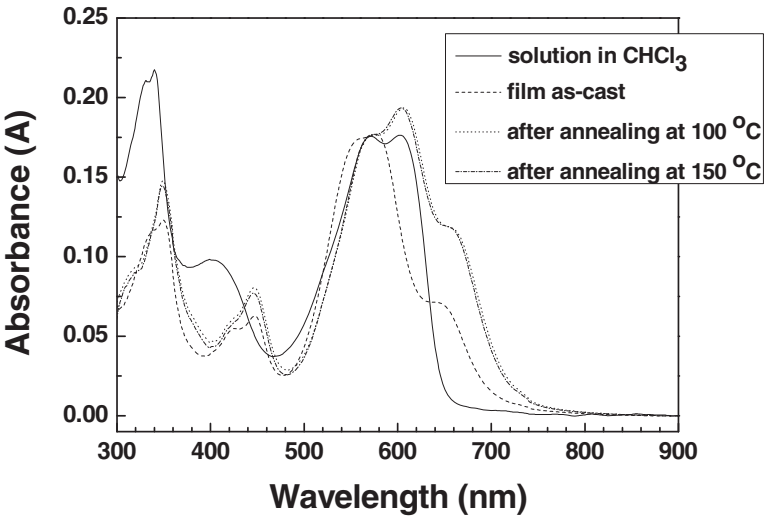

Figure 1. UV-Vis spectra of the PCTDPP20 in $CHCl_3$ (straight line), as-cast film (dash line) and annealed at 100°C (dot line) and 150°C (dash-dot line).

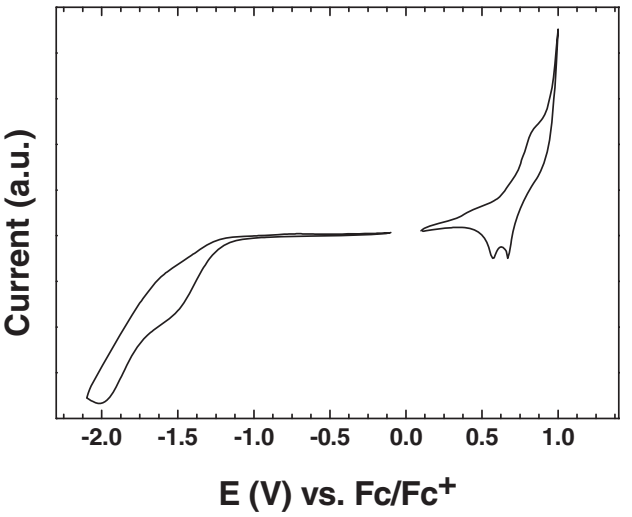

Figure 2. Cyclic voltammogram of the PCTDPP20 film in a 0.10 M Bu_4NPF_6/CH_3CN solution at a scan rate of 100 mV/s.

As shown in Figure 2, the PCTDPP20 shows two oxidation and reduction peaks and has irreversible process. The reduction and oxidation onset potential appear at -1.23 and 0.23 V vs Fc/Fc^+, and the calculated the HOMO and LUMO energy levels are −5.13 and −3.57 eV, respectively. From cyclic voltammogram, we confirm that the

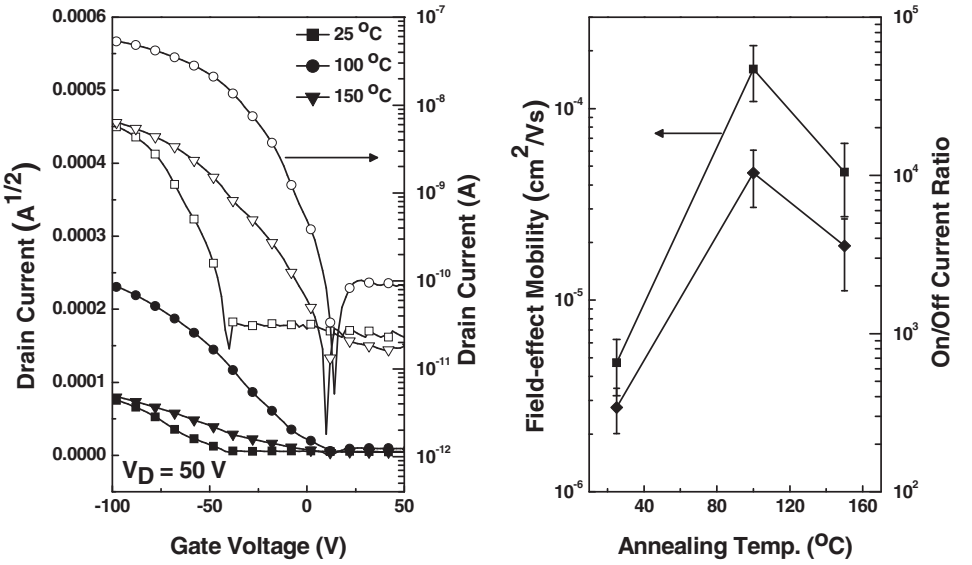

Figure 3. (a) p-type transfer characteristics curves (drain current (I_D)-gate voltage (V_G)) of OFETs based on PCTDPP20 at room temperature (square), and after annealing at 100°C (circle) and 150°C (triangle). (b) field-effect mobility (square) and on/off current ratio (diamond) of the OFETs as a function of temperature.

Table 2. OFET characterization with different annealing temperature

Annealing Temp. (°C)	μ_h (cm^2/Vs)[a]	$I_{on/off}$	V_{th} (V)[b]
25	4.7×10^{-6} ($\pm$ 1.542×10^{-6})	3.4×10^2 ($\pm$ 1.1×10^2)	−40
100	1.6×10^{-4} ($\pm$ 5.220×10^{-5})	1.0×10^4 ($\pm$ 4.1×10^3)	14
150	4.7×10^{-5} ($\pm$ 1.932×10^{-5})	3.6×10^3 ($\pm$ 1.7×10^2)	10

[a] hole mobility. [b] threshold voltage.

PCTDPP20 has suitable the HOMO and LUMO energy levels to apply active material of OSCs. The optical and electrochemical properties of the PCTDPP20 are listed in Table 1.

To investigate the hole mobility on thermal annealing process, fabricated OFETs carried out thermal annealing processes at 100°C and 150°C. Figure 3 exhibits the p-type transfer characteristics curves and average field-effect mobility and on/off current ratio (I_{on}/I_{off}) of the OFETs as a function of temperature. The transfer characteristics permit calculation of the field-effect mobility in the saturation regime ($V_D = -50$ V) using the relationship of $I_D = C_i W \mu (V_G - V_{th})^2/2L$, where W and L are the channel width and length, respectively, C_i the specific capacitance of the gate dielectric, and the μ field-effect mobility [16]. As-cast film presents a hole mobility of 4.7×10^{-6} cm^2/Vs, an I_{on}/I_{off} of 3.4×10^2 and a threshold voltage (V_{th}) of −40 V, performances of OFETs increase by thermal annealing. Between two annealing temperature, annealing the OFET at 100°C lead to improve a hole mobility up to 1.6×10^{-4} cm^2/Vs with a I_{on}/I_{off} (1.0×10^4) and a V_{th} (14 V). Surprisingly, the hole mobility of OFET annealed at 150°C are lower than those of OFET annealed at 100°C, while the shape absorption spectrum of the film annealed at 150°C is very similar to that of the film annealed at 100°C. At higher than critical temperature, 2-octyldodecyl side chains start to become softened and the layer-by-layer lamella crystalline structure

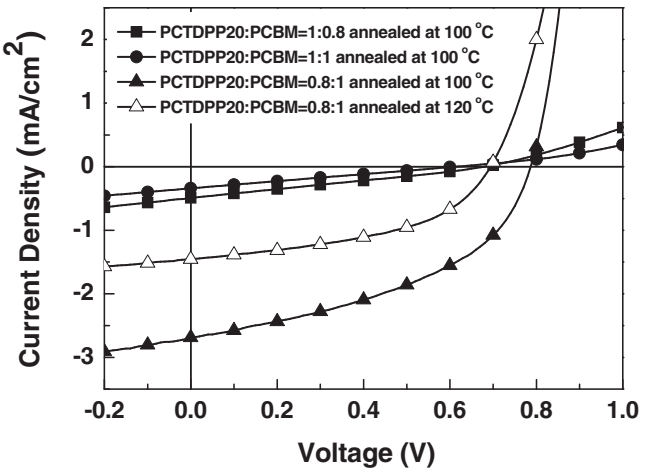

Figure 4. J-V characteristics of OSCs annealed at 100°C with blend ratios of 0.8:1 (filled square), 1:1 (filled circle) and 1:0.8 (filled triangle), and OSC annealed at 120°C with blend ratios of 1:0.8 (empty triangle).

Table 3. The photovoltaic parameters and efficiencies of OSCs with various blend ratios

PCTDPP: $PC_{60}BM$ Ratio	Annealing Temp. (°C)	J_{sc} (mA/cm^2)	V_{oc} (V)	FF (%)	PCE (%)
0.8: 1	100	−0.49	0.68	26.3	0.09
1: 1	100	−0.34	0.61	24.7	0.05
1: 0.8	100	−2.69	0.79	44.5	0.95
1: 0.8	120	−1.46	0.69	47.5	0.48

is partially destroyed, which is reported by Y. Li et al [20]. In our case, reduced the hole mobility at annealing 150°C seems to be cause by less crystalline structure than at annealing 100°C. And parameters of OFETs with different annealing temperature are listed in Table 2.

To optimize the blend ratio of PCTDPP20 and $PC_{60}BM$, we fabricated OSCs with different blend ratios from 0.8:1 to 1: 0.8. And based on OFET data, thermal annealing process of OSCs were carried out at 100°C for 10 min in glove box. As shown in Figure 4, the photovoltaic parameters and PCEs of OSCs are listed in Table 3. The OSCs with blend ratio of 1: 0.8 and 1:1 show negligible PCEs due to the absence of diode characteristics. The J_{sc} of these OSCs is very low value below 0.5 mA/cm^2 and V_{oc} values (0.68 and 0.61 V) are relatively lower than OSC with blend ratio of 1: 0.8 (0.79 V). This is due to the leakage current, charge carrier recombination or energy barrier between layers, which may be caused by poor film morphology such as unsuitable domain size, interpenetration between D and A, and so on [21–23]. Among the OSCs, device with blend ratio of 1: 0.8 shows the highest PCE of 0.95%, a J_{sc} of −2.69 mA/cm^2, a V_{oc} of 0.79 V and a fill factor of 44.5%. Additionally to check the optimum annealing temperature, we also fabricated OSC which was kept blend ratio of 1: 0.8 and annealed at 120°C for 10 min. As shown in Table 3, with increasing the annealing temperature from 100°C to 120°C, the PCE of OSC decreased almost in half. It is indicating that the optimized annealing temperature was at 100°C. This result coincides with the results of OFETs.

4. Conclusions

We synthesized a small molecule PCTDPP20 with 2,5-bis(2-octyldodecyl)-3,6-di(thiophen-2-yl)pyrrolo[3,4-c]pyrrole-1,4(2*H*,5*H*)-dione and 9-phenyl-9*H*-carbazole through the Suzuki coupling reaction. The PCTDPP20 film shows strong absorption between 500 ∼ 800 nm the after thermal annealing process. And the HOMO and LUMO energy levels of the PCTDPP20 are −5.13 and −3.57 eV, respectively. OFET annealed at 100°C presents the highest hole mobility of 1.6×10^{-4} cm^2/Vs. The best-performing OSC has generated a PCE of 0.95% with a J_{sc} of −2.69 mA/cm^2, a V_{oc} of 0.79 V and a fill factor of 44.5%.

Acknowledgment

This work was supported by a Research Grant of Pukyong National University (2013 year).

References

[1] Yu, G., Gao, J., Hummelen, J., Wudl, F., & Heeger, A. (1995). *SCIENCE.*, *270*, 1789.
[2] He, Z., Zhong, C., Su, S., Xu, M., Wu, H., & Cao, Y. (2012). *Nature Photonics.*, *6*, 593.
[3] Chen, J. J., Chen, T. L., Kim, B., Poulsen, D. A., Mynar, J. L., Fréchet, J. M., & Ma, B. (2010). *ACS Appl. Mater. Interfaces.*, *2*, 2679.
[4] Mazzio, K. A., Yuan, M., Okamoto, K., & Luscombe, C. K. (2011). *ACS Appl. Mater. Interfaces.*, *3*, 271.
[5] Mei, J., Graham, K. R., Stalder, R., & Reynolds, J. R. (2010). *Org. Lett.*, *12*, 660.
[6] Dutta, P., Kim, J., Eom, S. H., Lee, W., Kang, I. N., & Lee, S. (2012). *ACS appl. Mater. interfaces.*, *4*, 6669.
[7] Sharma, G., Mikroyannidis, J., Kurchania, R., & Thomas, K. J. (2012). *J. Mater. Chem.*, *22*, 13986.
[8] Huo, L., Hou, J., Chen, H., Zhang, S., Jiang, Y., Chen, T. L., & Yang, Y. (2009). *Macromolecules.*, *42*, 6564.
[9] Bijleveld, J. C., Zoombelt, A. P., Mathijssen, S. G., Wienk, M. M., Turbiez, M., de Leeuw, D. M., & Janssen, R. A. (2009). *J. Am. Chem. Soc.*, *131*, 16616.
[10] Sun, Y., Chien, S., Yip, H., Chen, K., Zhang, Y., Davies, J. A., Chen, F., Lin, B., & Jen, A. K. (2012). *J. Mater. Chem.*, *22*, 5587.
[11] Sonar, P., Ng, G., Lin, T. T., Dodabalapur, A., & Chen, Z. (2010). *J. Mater. Chem.*, *20*, 3626.
[12] Yiu, A. T., Beaujuge, P. M., Lee, O. P., Woo, C. H., Toney, M. F., & Fréchet, J. M. (2012). *J. Am. Chem. Soc.*, *134*, 2180.
[13] Huo, L., Hou, J., Chen, H., Zhang, S., Jiang, Y., Chen, T. L., & Yang, Y. (2009). *Macromolecules.*, *42*, 6564.
[14] Hwang, M. C., Jang, J., An, T. K., Park, C. E., Kim, Y., & Kwon, S. (2012). *Macromolecules.*, *45*, 4520.
[15] Chen, B., Ding, J., Wang, L., Jing, X., & Wang, F. (2012). *Chem.Commun.*, *48*, 8970.
[16] Shin, W., Jo, M. Y., You, D. S., Jeong, Y. S., Yoon, D. Y., Kang, J., Cho, J. H., Lee, G. D., Hong, S., & Kim, J. H. (2012). *Synth. Met.*, *162*, 768.
[17] Wang, X., Sun, Y., Chen, S., Guo, X., Zhang, M., Li, X., Li, Y., & Wang, H. (2012). *Macromolecules.*, *45*, 1208.
[18] Leliége, A., Blanchard, P., Rousseau, T., & Roncali, J. (2011). *Org. Lett.*, *13*, 3098.
[19] Takemoto, K., Karasawa, M., & Kimura, M. (2012). *ACS appl. Mater. interfaces.*, *4*, 6289.
[20] Li, Y., Sun, B., Sonar, P., Singh, S. P. (2012). *Organic Electronics*, *13*, 1606.
[21] Brabec, C. J., Heeney, M., McCulloch, I., & Nelson, J. (2011). *Chem. Soc. Rev.*, *40*, 1185.
[22] Jeong, W., Lee, J., Park, S., Kang, J., & Kim, J. (2011). *Adv. Funct. Mater.*, *21*, 343.
[23] Zhang, Y., Dang, X., Kim, C., & Nguyen, T. (2011). *Adv. Energy Mater.*, *1*, 610.